Supplement of Clim. Past Discuss., 11, 63–93, 2015
http://www.clim-past-discuss.net/11/63/2015/
doi:10.5194/cpd-11-63-2015-supplement

Climate of the Past
Discussions
Open Access

Supplement of

Strong winter monsoon wind causes surface cooling over India and China in the Late Miocene

H. Tang et al.

Correspondence to: H. Tang (hui.tang@helsinki.fi)

1. Model setup for the Late Miocene simulations

For the Late Miocene global model simulation (GLMio), the orography is generally lower than at present. In particular, the Tibetan Plateau (TP) is generally reduced to 70% of present- day height. The land–sea distribution is largely the same as today. But Australia is two grid cells southward compared to GCTRL. This leads to an open Indonesian Seaway. There is also an open Panama Isthmus with a depth of 500 m in the ocean model of GLMio. In addition, the Paratethys Sea and the Pannonian Lake in Central Eurasia are present. The CO2 concentration is set to 360 ppm which is equivalent to present. More details on the setup of the boundary conditions for the Late Miocene can be found in our previous studies (Micheels et al., 2011; Tang et al., 2013a). The GLMio was integrated over 2,600 years so that the model runs are in their dynamic equilibrium in terms of global mean temperature and sea ice volume. Here we use the last 110-year model integrations for analysis.

For the regional model simulation (RLMio), the initial and lateral boundary forcing are from the 6-hourly output of 110-year GLMio run. The physical boundary conditions were modified to be consistent with GLMio and to better represent the regional details of the Late Miocene conditions in the Asian monsoon region. As to palaeorography, we kept the elevations of the Himalayas and southern TP at their present-day heights (Coleman and Hodges, 1995; Rowley et al., 2001; Spicer et al., 2003; Polissar et al., 2009), but reduced the central and southeastern TP to 80% (Blisniuk et al., 2001; Liu-Zeng et al., 2008; Quade et al., 2011) and the northern TP to 30% of their present-day heights (H.B.Zheng et al., 2000; D.W.Zheng et al., 2006; Wang et al., 2008). The atmospheric CO2 concentration is also set to 360 ppm, which is identical to our global climate run. RLMio was integrated for 110 year. Since the initial adaptation of the upper-level soil moisture in the regional model requires several months (Tang et al., 2011), the first year integration is left for the model to spin up. Only the last 109-year results were analysed. More details on the regional model set up and the validation of our regional model experiments in comparison with observation and proxy data, can be found in our previous study (Tang et al., 2011).

2. The hagamann distance based on fuzzy logic

In this method, the uncertainties of the proxy reconstruction or modern observation (i.e. a fuzzy number) are considered by assuming a membership function for the fuzzy number:

$$h(x) = \begin{cases} L(x) = 1 - \left(\frac{a-x}{a-a_-}\right)^p & x \in [a_-, a] \\ R(x) = 1 - \left(\frac{x-a}{a_+-a}\right)^q & x \in [a, a_+] \\ 0 & otherwise \end{cases} \qquad (1)$$

where a_- and a_+ denote the smallest and largest values of a fuzzy number. a denotes the value which membership is 1 (i.e., pivot of a fuzzy number). The exponents p and q are positive real numbers which determine how sharp the membership function curves are. The large values for both exponents (*p,*

q >1) give a "fat" fuzzy number, indicating that each value in the range [a_-, a_+] is highly possible to be the "true value". In contrast, p, q <1 produce a "slim" fuzzy number, indicating that only the values near a are highly possible to be the "true value". When both exponents equal 1 (i.e., p=q=1), the membership function is triangle.

The difference between two fuzzy numbers (A and B) is then defined by the weighted average squared distance of both their left and right sides (i.e., Hagaman distance) as the following equation:

$$D^2(A,B) = \int_0^1 (L_a^{-1}(h) - L_b^{-1}(h))^2 + (R_a^{-1}(h) - R_b^{-1}(h))^2 h dh \qquad (2)$$

Where $L_{a\ or\ b}^{-1}(h)$ and $R_{a\ or\ b}^{-1}(h)$ are the inverse functions of $L(x)$ and $R(x)$ in equation (1) for fuzzy number A or B. h denotes the degree of membership and is in the range [0,1].

For plant fossil reconstruction, which gives the coexistence temperature interval, e.g., [Tmin, Tmax], we assume a, a_- and a_+ in equation (1) as follows

a=(Tmin+Tmax)/2; a_-=Tmin; a_+=Tmax;

Since any values in [Tmin, Tmax] are almost equally possible to be the true values, we assume p, q in equation (1) to be 20.

For modern observation data, we assume *a* as the average value of a climate variable (e.g., temperature), a_- and a_+ as the minimum and maximum value of that climate variable observed, respectively. Since the true value is more likely to lie around the average value in modern observation data, we simply assume *p, q* in equation (1) to be 1 (i.e., a triangle membership function). The modern observation is based on CRU TS 2.10 data set (1901-2002) (http://www.cru.uea.ac.uk/cru/data/hrg/cru_ts_2.10/) for the plant fossil data, and WorldClim data set (http://www.worldclim.org/current) for the mammal fossil data.

Since the mammal fossil reconstruction is based on linear regression method that gives the "best" estimations of climate variables, we simply use the difference between the fossil reconstructed temperature and the average value of modern observed temperature to depict the changes from the Late Miocene to the present. For plant fossil localities which are within 2° by 2° longitude-latitude grid, the data are synthesized to give an estimate for the whole grid. The synthesis is done by overlapping the climate intervals of different localities. This is consistent with the Coexistence Approach (CA) from which the original data are derived. For mammal fossil data, the synthesis is simply done by averaging the values from different localities within the 3° by 3° grid.

3. Temperature reconstructions based on plant and mammal fossil data

Table S1. The temperature reconstruction in the Late Miocene plant fossil localities and its comparison with the present-day values derived from CRU TS 2.10 dataset (1901-2002) (http://www.cru.uea.ac.uk/cru/data/hrg/cru_ts_2.10/). MAT: mean annual temperature; CMT: coldest month temperature; WMT: warmest month temperature. The localities showing cooler-than-present MAT or CMT in the Late Miocene are highlighted by yellow colour. Note that only the reconstructions using the Coexistence Approach (CA) are displayed in Fig. 3.

Locality names	Type of flora	Lat.	Long.	MAT	Range	CMT	Range	WMT	Rang	Method	References
Upper Minghuazhen, Bohai, China	Pollen	39.00	119.00	12.60	3.50	2.55	5.25	22.45	3.15	CA	Liu et al. (2011)
				11.19	2.77	-5.20	7.39	25.68	4.02		Modern
Upper Minghuazhen, Shandong, China	Pollen	36.97	117.20	15.00	3.40	6.10	6.40	25.60	2.60	CA	Liu et al. (2011)
				13.63	2.66	-2.34	6.41	27.34	4.04		Modern
Huanghua, Hebei, China	Pollen	41.50	117.00	15.90	0.20	6.05	1.05	24.80	0.10	CA	Liu et al. (2011)
				2.58	2.99	-15.88	7.80	18.74	4.38		Modern
Dadaiqiao, Heilongjiang, China	Pollen	47.00	130.00	15.05	1.05	3.30	3.80	25.15	0.45	CA	Liu et al. (2011)
				0.22	3.82	-23.02	9.53	19.98	4.28		Modern
Dunhuang, Gansu, China	Pollen	40.00	94.70	14.30	1.80	4.25	3.55	25.25	0.35	CA	Liu et al. (2011)
				9.13	3.28	-8.94	7.77	24.18	5.18		Modern
Shanwan-Taxihe, Xinjiang, China	Pollen	44.50	85.50	17.05	1.35	8.15	4.35	24.90	3.20	CA	Liu et al. (2011)
				8.93	4.13	-13.84	10.15	26.63	4.45		Modern
Xianshuihe, Qinghai, China	Pollen	36.40	102.20	15.55	6.15	7.75	7.85	23.45	4.65	CA	Liu et al. (2011)
				3.58	2.57	-9.47	5.55	14.82	4.53		Modern

Wulong a, Namling, China	Pollen	29.43	89.00	14.70	2.80	4.75	6.10	24.20	2.80	CA	Yao et al. (2011)
Wulong b, Namling, China	Pollen	29.43	89.00	15.90	0.40	5.80	4.00	24.20	2.80	CA	Yao et al. (2011)
Wulong c, Namling, China	Pollen	29.43	89.00	17.05	7.50	7.50	11.60	25.45	5.30	CA	Yao et al. (2011)
				2.77	2.18	-7.48	5.61	11.89	2.84		Modern
Lawula 1, Markam, China	Macroflora	29.00	98.00	15.10	7.80	5.45	14.10	26.15	4.30	CA	Yao et al. (2011)
Lawula a, Markam, China	Pollen	29.00	98.00	14.70	2.80	4.75	6.10	24.20	2.80	CA	Yao et al. (2011)
				2.82	1.83	-5.25	3.35	10.51	3.60		Modern
Dingqing 2, Lunpola Basin, China	Pollen	32.30	90.00	18.50	5.60	8.55	9.50	24.90	6.40	CA	Yao et al. (2011)
				-2.90	2.05	-14.50	6.56	8.06	4.21		Modern
Fushan 3, Fushan Depression, China	Pollen	19.50	109.56	18.45	5.70	11.45	3.70	26.40	3.40	CA	Yao et al. (2011)
				24.08	2.49	17.52	6.65	28.57	3.59		Modern
Leizhou 3, Leizhou Peninsul, China	Pollen	21.45	110.00	18.45	5.70	10.70	8.20	26.40	3.40	CA	Yao et al. (2011)
				23.25	1.99	14.99	7.45	29.02	1.89		Modern
Beibuwan 3, Beibuwan Depression, China	Pollen	20.30	108.30	18.45	5.70	12.20	5.20	28.10	0.00	CA	Yao et al. (2011)
				24.76	2.35	17.79	6.43	29.39	2.64		Modern
Yinggehai 3, Yinggehai Depression, China	Pollen	18.31	108.42	16.60	3.60	8.25	13.10	28.10	0.00	CA	Yao et al. (2011)
				25.41	2.77	19.90	5.20	29.13	7.07		Modern
Zhujiangkou 3, Zhujiangkou Basin, China	Pollen	22.25	113.45	22.00	0.00	14.55	0.50	28.10	0.00	CA	Yao et al. (2011)
				22.67	1.70	14.39	6.70	28.72	2.08		Modern
Arunachal Pradesh, India	Wood	27.60	94.70	26.10	1.60	22.60	5.20	28.10	0.00	CA	New reconstruction besed on Mehrotra et al. (1999)
				21.90	2.18	14.44	3.54	27.41	2.50		Modern

Assam, India	Wood	27.30	94.60	26.70	0.40	23.15	4.10	28.30	0.40	CA	New reconstruction besed on Mehrotra et al. (2011)
				23.27	2.23	15.97	3.44	28.58	2.57		Modern
Danzengzhukang Fm, Gyirong Basin, China	Pollen	28.75	85.30	17.45	1.90	6.65	2.30	27.70	0.80	CA	New reconstruction based on Xu et al. (2012)
				-6.54	2.45	-15.80	3.96	2.77	2.92		Modern
Dupi Tila, Bengladash	Pollen	25.50	88.96	24.55	1.90	19.05	4.70	27.60	0.60	CA	New reconstruction based on Li and Zhang (2000)
				25.07	2.13	17.52	3.91	29.35	2.48		Modern
Jharkhand, India	Macroflora	23.40	84.10	26.80	0.60	21.45	4.10	28.10	0.00	CA	New reconstruction based on Singh and Prasad (2007)
				23.12	2.51	14.79	4.45	30.99	5.72		Modern
Khorat, Thailand	Pollen	15.02	102.27	22.25	1.70	16.95	0.10	27.50	0.40	CA	New reconstruction based on Sepulchre et al. (2010)
				27.22	2.70	22.48	5.23	30.32	3.70		Modern
Lower Woma Fm, Gyirong Basin, China (7.2-3.2 Ma)	Pollen	28.75	85.30	18.65	4.30	6.65	2.30	27.70	0.80	CA	New reconstruction based on Xu et al. (2012)
				-6.54	2.45	-15.80	3.96	2.77	2.92		Modern
Surai Khola, Nepal (11.5-8 Ma)	Pollen	27.80	82.81	20.05	2.50	13.45	0.30	27.60	0.60	CA	New reconstruction

											based on Hoorn et al. (2000)
Surai Khola, Nepal (8-6 Ma))	Pollen	27.80	82.81	19.90	2.80	10.50	5.60	27.60	0.60	CA	New reconstruction based on Hoorn et al. (2000)
Surai Khola, Nepal (6-5 Ma)	Pollen	27.80	82.81	22.85	1.30	17.50	7.80	28.10	0.00	CA	New reconstruction based on Hoorn et al. (2000)
				22.85	2.54	13.73	3.86	29.20	3.58		Modern
Xianfeng, Yunan, China	Macroflora	25.42	102.85	19.45	4.50	11.85	2.30	24.75	2.70	CA	Xing et al. (2012)
Xianfeng, Yunan, China	Macroflora	25.42	102.85	17.32	4.92					LMA	Xing et al. (2012)
Xianfeng, Yunan, China	Macroflora	25.42	102.85	15.43	2.50	6.23	5.14	26.78	3.02	CLAMP	Xing et al. (2012)
				14.36	2.18	6.97	5.67	19.95	2.30		Modern
Lingcang 1, Yunan, China	Macroflora	23.90	100.02	18.75	0.50	10.10	2.90	27.55	0.50	CA	Jacques et al. (2011)
Lingcang 1, Yunan, China	Macroflora	23.90	100.02	20.60	2.40	11.40	3.80	29.00	3.20	CLAMP	Jacques et al. (2011)
Lingcang 2, Yunan, China	Macroflora	23.90	100.02	19.80	2.50	11.20	5.14	27.30	3.02	CLAMP	Xing et al. (2012)
				16.72	2.05	10.39	3.15	21.23	3.20		Modern
Xiaolongtan 1, Yunnan, China	Macroflora	23.48	103.11	20.70	0.20	10.20	9.20	27.65	0.90	CA	Yao et al. (2011)
Xiaolongtan 2, Yunnan, China	Macroflora	23.80	103.20	17.95	2.50	8.20	1.00	25.70	0.60	CA	Xia et al. (2009)
Xiaolongtan 2, Yunnan, China	Macroflora	23.80	103.20	22.30	2.05					LMA	Xia et al. (2009)
Xiaolongtan 2, Yunnan, China	Macroflora	23.80	103.20	18.10	2.40	10.80	3.80	25.90	3.20	CLAMP	Xia et al. (2009)
Xiaolongtan 3, Yunnan, China	Macroflora	23.80	103.20	19.90	2.50	12.50	5.14	26.70	3.02	CLAMP	Xing et al. (2012)
				16.50	3.10	9.35	5.71	21.54	3.62		Modern
Lühe, Yunnan, China	Pollen	25.17	101.37	17.10	7.60	7.50	10.10	25.00	5.00	CA	Xu et al. (2008)
Lühe 1, Yunnan, China	Pollen	25.10	101.22	17.60	8.60	7.75	15.70	25.45	5.30	CA	Yao et al. (2011)

Lühe 2, Yunnan, China	Pollen	25.10	101.22	15.40	4.20	3.80	7.80	25.45	4.90	CA	Yao et al. (2011)
Lühe 5, Yunnan, China	Pollen	25.10	101.22	15.40	12.60	6.45	18.30	23.70	8.80	CA	Yao et al. (2011)
Lühe 10, Yunnan, China	Pollen	25.10	101.22	16.60	10.20	7.30	16.60	25.65	5.30	CA	Yao et al. (2011)
Lühe 16, Yunnan, China	Pollen	25.10	101.22	16.60	10.20	7.30	16.60	25.55	5.10	CA	Yao et al. (2011)
Lühe 18, Yunnan, China	Pollen	25.10	101.22	15.00	6.80	6.10	12.80	25.45	4.90	CA	Yao et al. (2011)
Lühe 22, Yunnan, China	Pollen	25.10	101.22	17.50	8.40	7.75	15.70	25.45	5.30	CA	Yao et al. (2011)
Lühe 23, Yunnan, China	Pollen	25.10	101.22	16.60	10.20	7.30	16.60	25.65	5.30	CA	Yao et al. (2011)
				16.14	2.13	8.85	5.19	21.72	2.82		Modern

Table S2. The temperature reconstruction in the Late Miocene mammal fossil localities and its comparison with the present-day values derived from WorldClim dataset (http://www.worldclim.org/current). MAT: mean annual temperature; CQT: coldest quarter temperature. The localities showing cooler-than-present MAT or CQT in the Late Miocene are highlighted by yellow colour. The mean hypsodonty (HYP) and mean longitudinal lophs (LOP) are from the NOW database (downloaded on 28.11.2012 from: http://www.helsinki.fi/science/now/). MAT and CQT are calculated based on the linear regression models found for present day by Liu et al. (2012): MAT=+24.730 +13.793*HYP -25.058*LOP (r^2=0.69); CQT=+26.249 +17.814*HYP -37.659*LOP (r^2=0.70). As illustrated by the equations, mammalian herbivore assemblages with high loph count and low hypsodonty are associated with cold environments and thus indicative of low temperature, and vice versa.

Lat.	Long.	Mean HYP	Mean LOP	MAT	MAT	CQT	CQT

				(Late Miocene)	(present)	(Late Miocene)	(present)
41.31	45.23	1.56	1.22	15.49	13.26	7.93	2.50
41.30	45.70	1.56	1.16	17.10	13.18	10.35	2.51
37.41	46.35	2.00	1.38	17.79	9.03	10.10	-2.62
47.00	92.60	2.29	1.69	13.89	-0.35	3.42	-20.43
47.00	92.40	2.13	1.22	23.35	-1.30	18.08	-20.54
37.00	97.00	2.00	1.75	8.38	4.53	-4.03	-8.39
42.36	112.74	1.00	1.50	0.85	4.15	-12.43	-13.88
31.56	93.83	2.25	1.80	10.57	-1.28	-1.46	-10.82
37.99	106.20	1.75	1.25	17.48	8.72	10.35	-5.86
37.49	105.66	2.33	1.00	31.80	8.40	30.16	-5.69
34.30	69.40	2.00	2.00	2.10	9.69	-13.44	-2.48
34.35	69.41	1.83	1.89	2.59	10.04	-12.23	-2.02
47.00	92.40	2.29	1.67	14.41	-1.30	4.20	-20.54
42.20	75.60	1.70	1.70	5.49	1.03	-7.49	-14.17
52.20	76.90	1.00	0.50	25.95	2.44	25.23	-15.81
41.10	70.00	2.33	1.67	15.07	7.81	5.05	-4.57
42.95	77.30	1.88	1.67	8.74	1.06	-3.11	-13.37
49.40	66.00	2.00	2.00	2.10	6.67	-13.44	-10.09
34.10	109.30	2.09	1.54	14.94	12.18	5.56	-0.02
41.31	45.23	1.80	1.40	14.40	13.26	5.59	2.50
41.30	45.70	2.33	1.33	23.43	13.18	17.60	2.51
41.31	45.21	1.80	1.40	14.40	13.15	5.59	2.40
41.31	45.21	2.50	1.50	21.55	13.15	14.30	2.40
45.38	101.51	2.00	1.00	27.20	2.74	24.22	-13.21

50.16	66.66	1.00	1.00	13.40	5.13	6.40	-11.89
50.16	70.50	1.67	1.43	11.84	2.78	2.14	-15.20
16.75	99.00	1.33	0.71	25.17	26.58	23.10	23.49
38.66	69.86	2.00	1.80	7.12	8.66	-5.91	-3.03
21.00	103.90	1.50	0.50	32.85	20.12	34.14	14.85
41.83	111.50	3.00	1.50	28.45	3.47	23.20	-14.31
35.61	103.61	3.00	1.50	28.45	6.17	23.20	-5.68
39.00	111.00	2.00	1.38	17.79	7.15	10.10	-8.49
34.00	109.00	2.00	1.67	10.47	11.92	-0.89	-0.02
34.00	109.00	2.67	2.00	11.30	11.92	-1.57	-0.02
34.00	109.00	1.00	0.50	25.95	11.92	25.23	-0.02
34.00	109.00	2.00	1.44	16.04	11.92	7.48	-0.02
34.00	109.00	2.00	1.50	14.65	11.92	5.39	-0.02
34.00	109.00	2.40	1.83	11.80	11.92	-0.04	-0.02
35.00	106.00	2.00	1.33	18.83	8.56	11.66	-3.03
39.00	111.00	1.79	1.69	6.99	7.15	-5.49	-8.49
33.40	109.10	1.83	1.74	6.41	10.94	-6.50	-0.04
19.96	95.14	1.00	0.00	38.50	27.03	44.06	22.37
22.93	94.10	1.32	0.81	22.62	22.29	19.31	17.37
35.83	103.75	2.57	1.25	28.81	6.92	24.98	-5.41
35.85	103.73	1.78	1.70	6.47	6.97	-6.24	-5.40
35.86	103.76	1.50	1.42	9.84	6.98	-0.38	-5.40
35.48	103.50	1.50	1.00	20.30	5.09	15.31	-6.32
37.08	97.25	1.86	1.43	14.47	4.60	5.53	-8.39
28.00	82.50	1.67	1.60	7.54	21.01	-4.32	13.32

30.06	70.06	1.67	1.25	16.33	21.69	8.87	10.89
31.83	49.66	3.00	2.00	15.90	21.97	4.37	10.01
31.52	76.63	1.29	0.00	42.44	21.58	49.15	13.06
28.00	82.50	1.00	0.00	38.50	21.01	44.06	13.32
35.37	103.21	1.00	1.00	13.40	2.59	6.40	-8.14
41.11	45.80	1.50	1.22	14.72	12.09	6.94	1.62
41.68	45.75	1.29	1.38	7.93	12.14	-2.63	1.64
37.40	46.33	2.25	2.00	5.55	9.14	-8.99	-2.53
37.40	46.33	2.50	1.75	15.27	9.14	4.88	-2.53
37.40	46.33	2.00	2.00	2.10	9.14	-13.44	-2.53
37.40	46.33	2.00	1.00	27.20	9.14	24.22	-2.53
20.32	78.85	1.00	2.00	-11.70	27.38	-31.26	22.03
47.40	84.95	2.00	1.82	6.66	1.94	-6.59	-15.35
20.10	95.11	1.20	0.58	26.62	27.09	25.66	22.43
47.30	85.30	2.11	1.80	8.65	-0.68	-3.93	-16.19
41.90	45.00	1.50	1.57	5.96	9.77	-6.21	-0.44
34.31	69.41	1.55	1.29	13.76	9.76	5.36	-2.37
37.40	46.36	1.93	1.73	8.03	9.10	-4.36	-2.56
37.40	46.41	1.89	1.63	9.89	9.03	-1.44	-2.60
52.00	77.00	2.15	1.73	10.92	2.56	-0.66	-15.63
49.20	93.40	2.30	1.85	10.10	-2.07	-2.30	-26.48
49.20	93.40	2.38	1.89	10.06	-2.07	-2.58	-26.48
45.40	100.90	2.00	1.25	20.92	2.52	14.80	-13.67
49.20	93.40	3.00	2.00	15.90	-2.07	4.37	-26.48
42.40	75.60	1.75	1.63	8.06	2.63	-3.77	-12.27

39.27	67.65	1.88	1.40	15.44	5.84	6.93	-4.98
50.30	79.16	1.88	1.63	9.79	3.38	-1.55	-14.43
34.10	109.30	1.67	1.33	14.23	12.18	5.73	-0.02
34.10	109.30	1.80	1.67	7.71	12.18	-4.45	-0.02
34.10	109.30	2.20	1.86	8.45	12.18	-4.50	-0.02
34.10	109.30	2.00	1.80	7.12	12.18	-5.91	-0.02
37.00	112.90	1.40	1.33	10.55	8.06	0.98	-5.56
25.30	102.40	1.00	0.86	16.82	15.58	11.54	9.51
24.16	52.56	2.00	1.22	21.62	27.23	15.85	19.05
29.03	69.15	1.67	1.67	5.87	23.77	-6.83	13.02
50.25	67.83	2.14	1.87	7.42	3.52	-5.87	-14.19
24.06	53.43	2.00	1.00	27.20	27.03	24.22	19.17
23.10	52.51	1.83	1.08	22.97	27.30	18.35	19.28
24.00	52.33	2.00	1.20	22.18	27.32	16.69	19.08
24.10	52.43	1.77	1.13	20.67	27.27	15.09	19.05
24.15	53.00	1.75	1.00	23.75	27.11	19.76	19.11
24.11	53.00	1.80	1.20	19.42	27.10	13.12	19.10
24.00	53.00	1.50	1.38	10.89	27.05	1.19	19.06
24.06	53.33	1.75	1.60	8.69	27.03	-2.83	19.14
34.00	109.00	2.00	1.82	6.66	11.92	-6.59	-0.02
15.00	102.33	1.70	0.82	27.62	26.99	25.72	23.84
38.35	46.11	2.40	1.63	17.03	10.13	7.81	-1.48
39.33	67.83	2.00	1.00	27.20	4.86	24.22	-6.02
35.05	108.05	1.00	0.00	38.50	10.77	44.06	-1.52
35.00	103.00	2.00	1.75	8.38	1.92	-4.03	-8.28

39.00	111.00	1.86	1.86	3.71	7.15	-10.61	-8.49
34.60	112.20	1.29	1.43	6.59	13.26	-4.65	0.23
42.00	114.00	1.60	1.67	4.95	3.42	-8.01	-13.49
42.00	114.00	1.50	1.75	1.48	3.42	-12.93	-13.49
28.86	85.18	1.86	1.88	3.27	-0.34	-11.28	-7.38
31.00	112.00	1.67	1.00	22.60	16.09	18.28	4.90
40.00	112.00	3.00	1.50	28.45	4.95	23.20	-10.60
40.00	112.00	1.86	1.89	2.92	4.95	-11.80	-10.60
36.00	108.00	2.00	1.75	8.38	9.23	-4.03	-3.47
36.00	108.00	2.10	2.00	3.48	9.23	-11.66	-3.47
34.00	109.00	1.75	1.56	9.81	11.92	-1.16	-0.02
34.00	109.00	1.00	1.00	13.40	11.92	6.40	-0.02
39.00	111.00	1.90	1.92	2.81	7.15	-12.08	-8.49
39.00	111.00	1.90	1.82	5.28	7.15	-8.38	-8.49
39.00	111.00	1.88	1.70	7.91	7.15	-4.37	-8.49
39.00	111.00	2.12	1.79	9.01	7.15	-3.42	-8.49
39.00	111.00	2.09	1.77	9.15	7.15	-3.13	-8.49
39.01	111.09	1.81	1.63	8.76	7.15	-2.91	-8.50
39.00	111.00	1.86	1.57	11.04	7.15	0.39	-8.49
39.00	111.17	1.53	1.57	6.32	7.13	-5.74	-8.52
39.00	111.00	1.71	1.33	14.89	7.15	6.58	-8.49
36.96	103.29	1.64	1.57	7.84	3.57	-3.78	-8.25
36.96	103.27	1.78	1.67	7.40	3.49	-4.85	-8.29
33.66	105.00	1.57	1.58	6.80	9.30	-5.14	-0.44
36.80	112.80	1.67	1.25	16.33	8.96	8.87	-4.71

36.80	112.90	1.43	1.75	0.49	8.73	-14.21	-4.94
36.80	112.90	1.43	1.71	1.39	8.73	-12.86	-4.94
36.80	112.90	1.25	1.67	0.12	8.73	-14.25	-4.94
36.66	117.46	1.50	1.50	7.75	13.62	-3.52	-0.39
39.00	111.00	1.45	1.55	5.98	7.15	-6.04	-8.49
24.16	52.56	1.53	1.21	15.48	27.23	7.98	19.05
24.07	52.70	1.67	1.00	22.60	27.16	18.28	19.04
44.33	112.87	2.00	2.00	2.10	2.03	-13.44	-17.39
35.50	103.50	1.67	1.00	22.60	5.21	18.28	-6.26
35.46	103.16	1.50	1.17	16.12	3.38	9.03	-7.64
35.33	103.16	1.60	0.83	25.86	2.19	23.37	-8.38
37.00	113.00	1.25	1.22	11.36	7.92	2.62	-5.69
34.00	111.00	1.40	1.57	4.58	10.93	-7.99	-0.90
35.50	105.66	1.50	1.40	10.26	7.75	0.25	-4.16
36.50	108.00	2.33	1.33	23.43	8.45	17.60	-4.58
34.08	105.08	2.00	1.00	27.20	8.77	24.22	-1.41
35.25	106.91	2.00	2.00	2.10	9.45	-13.44	-2.53
45.00	81.00	2.33	1.80	11.72	-4.04	0.03	-19.37
36.48	111.66	1.67	1.50	10.05	10.74	-0.55	-2.76
36.00	101.50	2.00	1.40	17.16	0.86	9.15	-10.01
39.33	94.33	2.00	1.80	7.12	0.52	-5.91	-12.59
37.75	118.08	3.00	1.50	28.45	12.60	23.20	-1.58
32.00	77.00	1.22	0.74	23.07	12.07	20.27	3.69
27.86	82.83	1.50	1.60	5.24	21.74	-7.28	13.97
27.00	85.00	2.33	1.00	31.80	24.24	30.16	16.58

38.00	69.50	2.00	2.00	2.10	14.05	-13.44	2.59
39.26	67.65	2.00	1.75	8.38	5.73	-4.03	-5.08
39.26	67.66	3.00	1.33	32.63	5.65	29.48	-5.16
49.00	93.00	2.50	2.00	9.00	-1.54	-4.53	-25.57
51.73	94.41	1.00	1.33	5.03	-3.75	-6.15	-26.64
37.04	112.99	1.00	0.67	21.77	7.81	18.96	-5.78
46.41	87.47	3.00	1.50	28.45	6.28	23.20	-12.58
37.40	46.33	1.83	2.00	-0.20	9.14	-16.41	-2.53
37.40	46.33	3.00	1.67	24.27	9.14	16.93	-2.53
37.40	46.33	2.00	1.89	4.89	9.14	-9.26	-2.53
37.40	46.33	2.50	2.00	9.00	9.14	-4.53	-2.53
37.40	46.33	1.73	1.64	7.46	9.14	-4.61	-2.53
37.40	46.33	2.00	2.00	2.10	9.14	-13.44	-2.53
37.40	46.33	3.00	2.00	15.90	9.14	4.37	-2.53
37.40	46.33	2.25	2.00	5.55	9.14	-8.99	-2.53
37.40	46.33	2.50	2.00	9.00	9.14	-4.53	-2.53
37.40	46.33	3.00	1.75	22.17	9.14	13.79	-2.53
37.40	46.33	2.50	2.00	9.00	9.14	-4.53	-2.53
37.40	46.33	2.25	2.00	5.55	9.14	-8.99	-2.53
37.40	46.33	1.83	1.67	8.17	9.14	-3.86	-2.53
37.40	46.33	2.00	1.67	10.47	9.14	-0.89	-2.53
37.40	46.33	2.09	1.73	10.20	9.14	-1.55	-2.53
37.40	46.33	3.00	2.00	15.90	9.14	4.37	-2.53
21.50	94.58	1.17	0.38	31.15	25.35	32.55	20.72
39.41	111.41	1.80	1.73	6.19	6.54	-6.73	-9.19

4. Sensitive experiments with the removal of the northern and southeastern Tibetan Plateau

Figure S1. Winter temperature (°C), 850 hPa wind (m/s) and sea level pressure (hPa) changes due to the removal of the northern and southeastern Tibetan Plateau (i.e., McTibet-MnTibet) under present-day (c) and Late Miocene global forcing (d). The orography for experiment McTibet and MnTibet are shown in (a) and (b). More details on the model set up of McTibet and MnTibet can be found in Tang et al. (2013b). In (c) and (d), the area dotted by grey colour has temperature anomalies significant with a Student's *t*-test ($p<0.05$). The black vectors indicate either the zonal or meridional wind differences are significant with a Student's *t*-test ($p<0.05$). The solid (dotted) green contours denote the positive (negative) sea level pressure anomalies due to the removal of the northern and southeastern Tibetan Plateau. Note that the effects of the northern and southeastern Tibetan Plateau on the winter monsoon are similar under the present-day and Late Miocene global forcings, indicating that such effects are insensitive to the global forcings of the regional model.

References

Blisniuk, P. M., Hacker, B. R., Glodny, J., Ratschbacher, L., Bi, S. W., Wu, Z. H., et al., 2001, Normal faulting in central Tibet since at least

13.5 Myr ago: Nature, v. 412, no. 6847, p. 628-632.

Coleman, M., and Hodges, K., 1995, Evidence for Tibetan Plateau uplift before 14 Myr ago from a new minimum age for east-west extension: Nature, v. 374, no. 6517, p. 49-52.

Hoorn, C., Ohja, T., and Quade, J., 2000, Palynological evidence for vegetation development and climatic change in the Sub-Himalayan Zone (Neogene, Central Nepal): Palaeogeography Palaeoclimatology Palaeoecology, v. 163, no. 3-4, p. 133-161.

Jacques, F. M. B., Guo, S.-X., Su, T., Xing, Y.-W., Huang, Y.-J., Liu, Y.-S., et al., 2011, Quantitative reconstruction of the Late Miocene monsoon climates of southwest China: A case study of the Lincang flora from Yunnan Province: Palaeogeography, Palaeoclimatology, Palaeoecology, v. 304, no. 3-4, p. 318-327.

Li, J. G., and Zhang, Y. Y., 2000, A Neogene palynoflora from the upper Dupi Tila (UDT) formation in Barapukulia coalmine, Bangladesh: Acta Palaeontologica Sinica, v. 39, no. 2, p. 189-196.

Liu, L., Puolamäki, K., Eronen, J. T., Ataabadi, M. M., Hernesniemi, E., and Fortelius, M., 2012, Dental functional traits of mammals resolve productivity in terrestrial ecosystems past and present: Proceedings of the Royal Society B: Biological Sciences, v. 279, no. 1739, p. 2793-2799.

Liu, Y. S., Utescher, T., Zhou, Z. K., and Sun, B. N., 2011, The evolution of Miocene climates in North China: Preliminary results of quantitative reconstructions from plant fossil records: Palaeogeography Palaeoclimatology Palaeoecology, v. 304, no. 3-4, p. 308-317.

Liu-Zeng, J., Tapponnier, P., Gaudemer, Y., and Ding, L., 2008, Quantifying landscape differences across the Tibetan plateau: Implications for topographic relief evolution: Journal of Geophysical Research, v. 113, no. F4.

Mehrotra, R. C., Awasthi, N., and Dutta, S. K., 1999, Study of fossil wood from the upper Tertiary sediments (Siwalik) of Arunachal Pradesh, India and its implication in palaeoecological and phytogeographical interpretations: Review of Palaeobotany and Palynology, v. 107, no. 3–4, p. 223-247.

Mehrotra, R. C., Bera, S. K., Basumatary, S. K., and Srivastava, G., 2011, Study of fossil wood from the Middle–Late Miocene sediments of Dhemaji and Lakhimpur districts of Assam, India and its palaeoecological and palaeophytogeographical implications: Journal of Earth System Science, v. 120, no. 4, p. 681-701.

Micheels, A., Bruch, A. A., Eronen, J., Fortelius, M., Harzhauser, M., Utescher, T., et al., 2011, Analysis of heat transport mechanisms from a Late Miocene model experiment with a fully-coupled atmosphere-ocean general circulation model: Palaeogeography Palaeoclimatology Palaeoecology, v. 304, no. 3-4, p. 337-350.

Polissar, P. J., Freeman, K. H., Rowley, D. B., McInerney, F. A., and Currie, B. S., 2009, Paleoaltimetry of the Tibetan Plateau from D/H ratios of lipid biomarkers: Earth and Planetary Science Letters, v. 287, no. 1–2, p. 64-76.

Quade, J., Breecker, D. O., Daëron, M., and Eiler, J., 2011, The paleoaltimetry of Tibet: An isotopic perspective: American Journal of Science, v. 311, no. 2, p. 77-115.

Rowley, D. B., Pierrehumbert, R. T., and Currie, B. S., 2001, A new approach to stable isotope-based paleoaltimetry: implications for paleoaltimetry and paleohypsometry of the High Himalaya since the Late Miocene: Earth and Planetary Science Letters, v. 188, no. 1-2, p. 253-268.

Sepulchre, P., Jolly, D., Ducrocq, S., Chaimanee, Y., Jaeger, J. J., and Raillard, A., 2010, Mid-Tertiary paleoenvironments in Thailand: pollen evidence: Clim. Past, v. 6, no. 4, p. 461-473.

Singh, S. K., and Prasad, M., 2007, Late Tertiary leaf flora of Mahuadanr Valley, Jharkhand: Journal of the Palaeontological Society of India, v. 52, no. 2, p. 175.

Spicer, R. A., Harris, N. B. W., Widdowson, M., Herman, A. B., Guo, S. X., Valdes, P. J., et al., 2003, Constant elevation of southern Tibet over the past 15 million years: Nature, v. 421, no. 6923, p. 622-624.

Tang, H., Eronen, J., Micheels, A., and Ahrens, B., 2013a, Strong interannual variation of the Indian summer monsoon in the Late Miocene: Climate Dynamics, v. 41, no. 1, p. 135-153.

Tang, H., Micheels, A., Eronen, J., Ahrens, B., and Fortelius, M., 2013b, Asynchronous responses of East Asian and Indian summer monsoons to mountain uplift shown by regional climate modelling experiments: Climate Dynamics, v. 40, no. 5-6, p. 1531-1549.

Tang, H., Micheels, A., Eronen, J., and Fortelius, M., 2011, Regional climate model experiments to investigate the Asian monsoon in the Late Miocene: Climate of the Past, v. 7, no. 3, p. 847-868.

Wang, Y., Wang, X. M., Xu, Y. F., Zhang, C. F., Li, Q., Tseng, Z. J., et al., 2008, Stable isotopes in fossil mammals, fish and shells from Kunlun Pass Basin, Tibetan Plateau: Paleo-climatic and paleo-elevation implications: Earth and Planetary Science Letters, v. 270, no. 1-2, p. 73-85.

Xia, K., Su, T., Liu, Y. S., Xing, Y. W., Jacques, F. M. B., and Zhou, Z. K., 2009, Quantitative climate reconstructions of the late Miocene Xiaolongtan megaflora from Yunnan, southwest China: Palaeogeography Palaeoclimatology Palaeoecology, v. 276, no. 1-4, p.

80-86.

Xing, Y., Utescher, T., Jacques, F. M. B., Su, T., Liu, Y., Huang, Y., et al., 2012, Paleoclimatic estimation reveals a weak winter monsoon in southwestern China during the late Miocene: Evidence from plant macrofossils: Palaeogeography, Palaeoclimatology, Palaeoecology, v. 358-360, p. 19-26.

Xu, J.-X., Ferguson, D. K., Li, C.-S., and Wang, Y.-F., 2008, Late Miocene vegetation and climate of the Lühe region in Yunnan, southwestern China: Review of Palaeobotany and Palynology, v. 148, no. 1, p. 36-59.

Xu, Y.-D., Zhang, K.-X., Wang, G.-C., Jiang, S.-S., Chen, F.-N., Xiang, S.-Y., et al., 2012, Extended stratigraphy, palynology and depositional environments record the initiation of the Himalayan Gyirong Basin (Neogene China): Journal of Asian Earth Sciences, v. 44, no. 0, p. 77-93.

Yao, Y.-F., Bruch, A. A., Mosbrugger, V., and Li, C.-S., 2011, Quantitative reconstruction of Miocene climate patterns and evolution in Southern China based on plant fossils: Palaeogeography, Palaeoclimatology, Palaeoecology, v. 304, no. 3–4, p. 291-307.

Zheng, D. W., Zhang, P. Z., Wan, J. L., Yuan, D. Y., Li, C. Y., Yin, G. M., et al., 2006, Rapid exhumation at similar to 8 Ma on the Liupan Shan thrust fault from apatite fission-track thermochronology: Implications for growth of the northeastern Tibetan Plateau margin: Earth and Planetary Science Letters, v. 248, no. 1-2, p. 198-208.

Zheng, H. B., Powell, C. M., An, Z. S., Zhou, J., and Dong, G. R., 2000, Pliocene uplift of the northern Tibetan Plateau: Geology, v. 28, no. 8, p. 715-718.

Figure S1

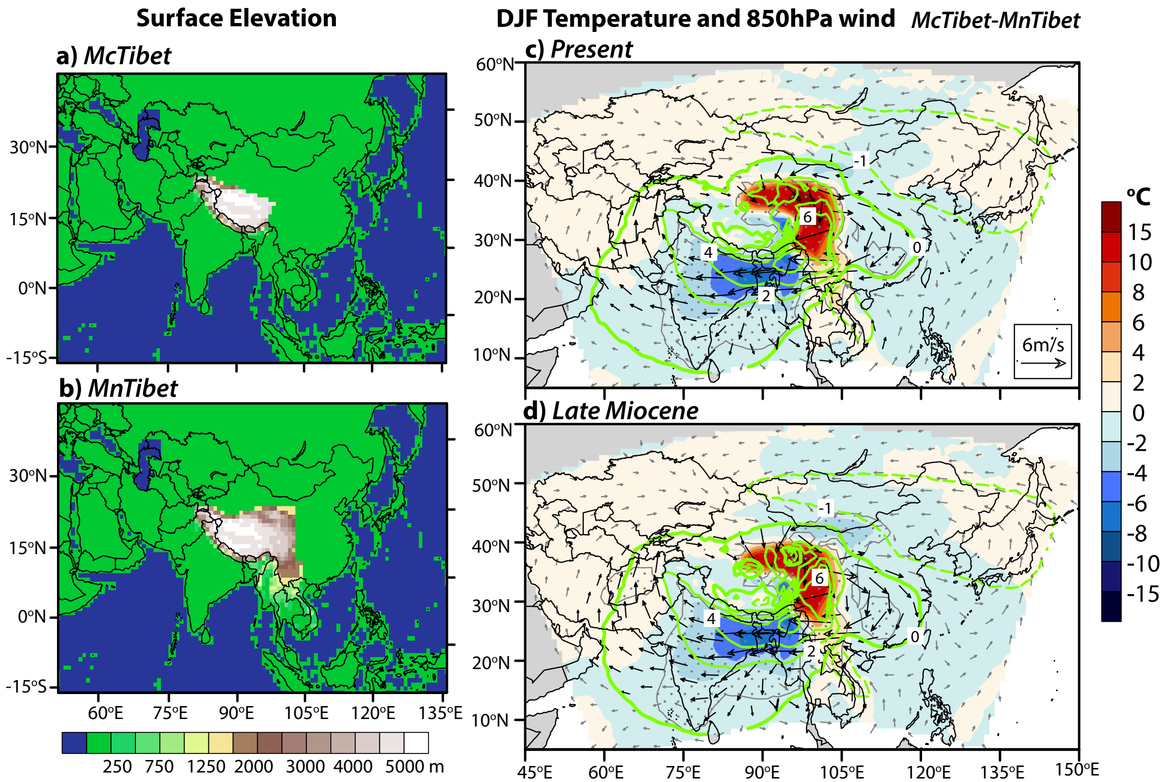

Surface Elevation
a) McTibet
b) MnTibet
30°N
15°N
0°N
-15°S
60°E
75°E
90°E
105°E
120°E
135°E
250
750
1250
2000
3000
4000
5000 m
DJF Temperature and 850hPa wind
McTibet-MnTibet
c) Present
d) Late Miocene
60°N
50°N
40°N
30°N
20°N
10°N
45°E
150°E
6m/s
°C
15
10
8
6
4
2
0
-2
-4
-6
-8
-10
-15